SOLITARY WAVE TRANSITION FROM LOW TO HIGH ENERGY IN THE FERMI–PASTA–ULAM LATTICE

Zhenying Wen†, Jun Tao, Nian Wei

College of Physics, Sichuan University, Chengdu 610065, China

(Received October 14, 2020; accepted June 28, 2021)

In this paper, we study analytically and numerically the solitary wave transition from low to high energy in localization, the relation between energy and velocity, propagation and scattering property in the Fermi–Pasta–Ulam lattice . When the energy of solitary wave increases to the threshold, the properties transform such as the width of solitary wave, the fluctuation of kinetic energy, the scattering effect after the head-on collision of two solitary waves, and the energy fluctuation after the scattering of a solitary wave and a discrete breather. The transition could help to understand the different chaotic dynamics of the Fermi–Pasta–Ulam lattice at low- and high-energy density.

DOI:10.5506/APhysPolB.52.1147

1. Introduction

The history of solitary waves can be traced back to 1834, when they were first discovered by Russell on the Union Canal in Scotland [1]. Several decades later, the Korteweg–de Vries equation was provided which explained the phenomenon mathematically [2]. More than a century later, Fermi, Pasta and Ulam (FPU) investigated the fundamental problem of energy equipartition and ergodicity in nonlinear systems and discovered FPU recurrence [3], which has led eventually to the soliton concept [4]. Since then, solitary waves have been studied in various different fields of physics such as solid-state physics, quantum theory, nonlinear optics, fluid dynamics, biophysics, *etc.* [5–13].

The transition of solitary waves from low to high energy is important in studies on energy transport. In the long-wavelength approximation, the FPU-α and FPU-β lattices lead to the KdV and modified KdV equations,

† Corresponding author: wenzy@scu.edu.cn

respectively, in which the soliton solutions exist. Solitary waves are deformed and energy exchange may occur when solitary waves interact with each other [14], and then make attribution to heat conduction [15, 16]. Up to now, very little work has been done on the study of transition and threshold of solitary waves in the FPU lattice, which may play a key role in heat conduction and diffusion process at temperatures varying from low to high.

In this work, we focus on the solitary wave transition from low to high energy in the FPU lattice. If the solitary wave, energy increases to the threshold, the transition takes place in the solitary wave localization, the fluctuation of kinetic energy, the energy loss rate after the head-on collision of two solitary waves, and the energy fluctuation after the scattering of a solitary wave and a discrete breather. The solitary wave properties become similar to those in the pure anharmonic lattice when energy tends to infinity. Finally the different chaotic dynamics of the FPU lattice at low- and high-energy density is discussed with the concept of solitary wave scattering.

2. Analysis in the weakly nonlinear limit

We consider the Hamiltonian for the FPU lattice

$$H = \sum_n H_n, H_n = \frac{p_n^2}{2} + V(q_{n+1} - q_n), \tag{1}$$

$$V(q) = \alpha q^2/2 + \beta q^4/4, \tag{2}$$

where p_n denotes the momentum and q_n denotes the displacement from equilibrium position for the n^{th} atom. Dimensionless units are used, such that the masses, the linear and nonlinear force constants, and the lattice constant are all chosen to be unity. The parameters α and β are the harmonic and anharmonic force constants, respectively. Here, $\alpha = 1$ and $\beta = 1$ for the FPU lattice throughout the paper.

The equations of motion of the FPU system are

$$\ddot{q}_n = (q_{n+1} - q_n) + (q_{n-1} - q_n) + (q_{n+1} - q_n)^3 + (q_{n-1} - q_n)^3. \tag{3}$$

In the long-wavelength limit, the continuum approximation should be applicable. The displacement $q_{n\pm1}$ of the $(n \pm 1)^{\text{th}}$ lattice is expanded as

$$q_{n\pm1} = q \pm q_x + \frac{1}{2}q_{xx} \pm \frac{1}{6}q_{xxx} + \frac{1}{24}q_{xxxx} + \dots, \tag{4}$$

where $q(x,t) = q_n(t)$, and $x = n$. Substituting Eq. (4) into Eq. (3) and neglecting higher-order terms, we obtain the continuous counterparts of Eq. (3)

$$q_{tt} = \left(1 + 3q_x^2\right) q_{xx} + \frac{1}{12}q_{xxxx}. \tag{5}$$

We shall be interested in right-going waves, and introduce the new slow variables

$$\xi = 2\varepsilon\,(x-t)\,, \qquad \tau = \varepsilon^3 t\,, \tag{6}$$

and define

$$q\,(x,t) = \varphi\,(\xi,\tau)\,, \tag{7}$$

where ε is a formal small parameter. Substituting Eqs. (6) and (7) into Eq. (5) and keeping terms in the order of ε^4, we obtain the following evolution equation for the $\psi = \partial\varphi/\partial\xi$ function:

$$\psi_\tau + \frac{3}{2}\psi^2\psi_\xi + \frac{1}{24}\psi_{\xi\xi\xi} = 0 \tag{8}$$

which is the well-known modified Korteweg–de Vries equation. Equation (8) is derived from the FPU chain [17, 18] and it results in the soliton solutions [19–21]

$$q_n \;=\; \varphi = -\sqrt{2/3}\arctan\left\{\mathrm{e}^{A\sqrt{6}\left[n-t-(A/2)^2 t\right]}\right\} + c\,, \tag{9}$$

$$p_n \;=\; \dot{q}_n = A\left[1+(A/2)^2\right]\operatorname{sech}\left\{A\sqrt{6}\left[n-t-(A/2)^2\,t\right]\right\}\,, \tag{10}$$

where c is constant. Equations (9) and (10) are valid if the higher derivatives are neglected. It can be achieved if the following is fulfilled:

$$6A^2 \ll 1\,. \tag{11}$$

The solutions for q_n and p_n are kink- and bell-shaped solitons, respectively, and the following soliton velocity is achieved:

$$v = 1 + (A/2)^2\,. \tag{12}$$

The soliton energy is

$$E = \sum_n \frac{p_n^2}{2} + \sum_n \left[(q_{n+1}-q_n)^2/2 + (q_{n+1}-q_n)^4/4\right]\,. \tag{13}$$

The first term of Eq. (13) denotes the kinetic energy of soliton and the second term is its potential energy. In the long-wavelength limit, the potential energy is very close to the kinetic energy for soliton at low energy, so soliton energy can be expressed as follows:

$$E = 2\sum_n \frac{p_n^2}{2}\,. \tag{14}$$

Since the soliton energy is unchanged as soliton propagates, substituting Eq. (10) at the time $t = 0$, we obtain

$$E = \sum_n \left\{ A \left[1 + (A/2)^2 \right] \operatorname{sech} \left(A\sqrt{6}n \right) \right\}^2 . \tag{15}$$

Replacing the sum by an integral in Eq. (15) due to continuum approximation and using Eq. (11), we finally arrive to

$$E = \frac{2}{\sqrt{6}} A \, . \tag{16}$$

Then we can get the relation between soliton energy and velocity from Eqs. (12) and (16) in the case of soliton energy $E \ll \frac{1}{3}$

$$v = 1 + \frac{3}{8} E^2 \, . \tag{17}$$

So the soliton velocity is close to the acoustic velocity due to the small energy.

3. Harmonic limit and anharmonic limit

We obtain the harmonic lattice in the absence of the quartic term, *i.e.*, $\alpha = 1$ and $\beta = 0$ for Eqs. (1) and (2). The system is integrable and can be analytically solved. Here, the acoustic velocity is 1.

It is the pure anharmonic lattice with $\alpha = 0$ and $\beta = 1$. In this case, the excitation, propagation and interaction of solitary waves have been studied in Refs. [16, 22, 23]. The system has an excellent scaling property, from which we can obtain the relation between energy E and velocity v of a solitary wave

$$v = a E^{1/4} \, , \tag{18}$$

where $a = 0.68198$ from numerical simulations [16].

4. Solitary wave transition from low to high energy in the FPU lattice

Solitary waves can be excited by momentum kicks on the lattice. We apply a kick p_1 on the first lattice at $t = 0$ for a static system under the free boundary condition. In Fig. 1, we plot p_i *versus* i after a short time ($t = 500$) for three kinds of lattices: the harmonic chain at $p_1 = 0.7$ (a), the pure anharmonic chain at $p_1 = 0.7$ (b), the FPU chain at $p_1 = 1.5$ (c) and the FPU chain at $p_1 = 0.7$ (d). In the harmonic chain, the amplitude of

the wave profile decreases, while the width increases with time continuously. In the pure anharmonic chain, a solitary wave is excited accompanied by the tail, which is made of several small solitary waves shown in the inset of Fig. 1 (b) [16]. In the FPU chain, at first, the wave front is connected with the other low amplitude excitations. If the imparted kick is large enough, after a certain short time, the wave front separates from the tail, because it moves faster. It propagates forward and becomes a solitary wave, just like that in Fig. 1 (c). The velocity v and energy E of the solitary wave excited by $p = 1.5$ are calculated numerically: $v = 1.139072$, $E = 1.040022$, and the relation of v and E does not satisfy Eq. (17). The solitary wave is localized on 9 lattices and the long-wavelength limit is not satisfied, so it is not consistent with the analytical results of Eqs. (17) and (9).

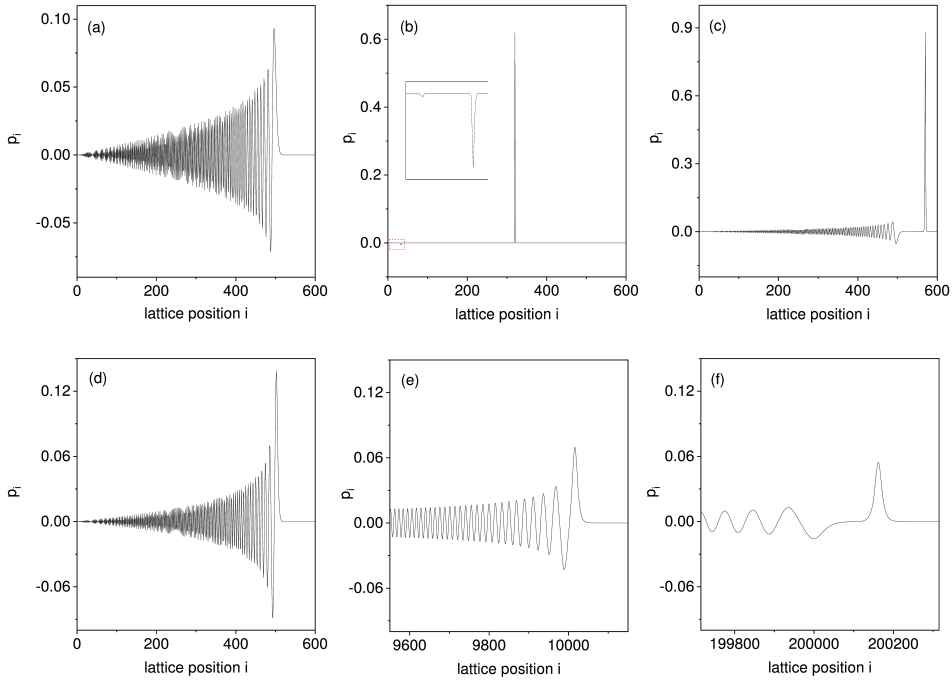

Fig. 1. The momentum p_i *versus* lattice position i. (a) the harmonic chain at $p_1 = 0.7$ and $t = 500$. (b) the pure anharmonic chain at $p_1 = 0.7$ and $t = 500$. (c) the FPU chain at $p_1 = 1.5$ and $t = 500$. (d), (e) and (f) represent the FPU chain at $p_1 = 0.7$ with $t = 500$, $t = 10^4$ and $t = 2 \times 10^5$, respectively.

If the kick is small, the excited wave packet looks like that in the harmonic chain in a short time (Fig. 1 (d), $p = 0.7$). However actually, it will show the essential difference after a long time. Consider the lattice which is so long that the wave packet will not reach the other end of the lattice in

the long observing time. As the first wave pulse travels, its width becomes wider and its peak becomes lower, as shown in Fig. 1 (e) at the time of $t = 10^4$, still like that in the harmonic chain. The speed of the first pulse is calculated and it is a little larger than the acoustic velocity of 1, and so it is not a linear wave. The first pulse travels a little faster than the second pulse, so as long as time is long enough, the first pulse will separate from the second one. Figure 1 (f) displays the separation of the first pulse from the others at $t = 2 \times 10^5$, and from then on its shape and energy do not changed any more, and it becomes a solitary wave. We obtain the numerical results: $v = 1.000743$, $E = 0.044664$, which satisfy the relation of Eq. (17). We present this solitary wave in the momentum space and configuration space in Fig. 2, which shows the solitary wave fits the Eqs. (10) and (9) excellently. A can be obtained from Eq. (12) (Eq. (16)) with v (E). The solitary wave is localized on about 72 lattices and the continuum approximation is applicable, so it satisfies the analytical results.

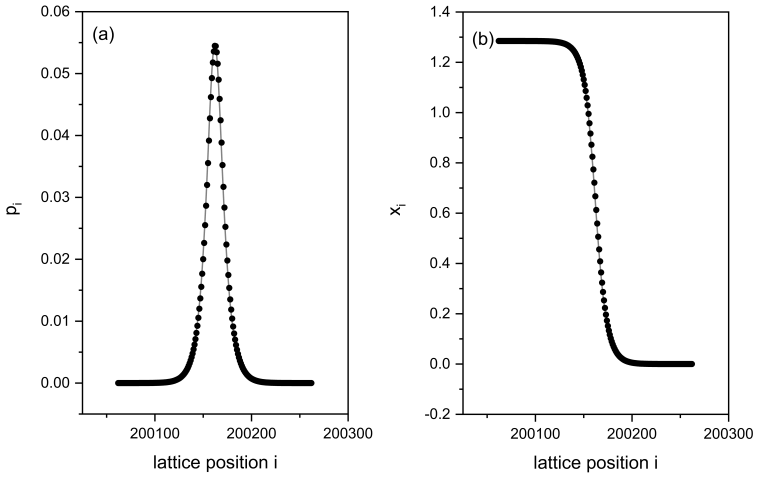

Fig. 2. Dots represent the solitary wave in Fig. 1 (f) in the momentum space (a) and configuration space (b). Solid lines in (a) and (b) stand for fitted curves of Eq. (10) and Eq. (9), respectively.

We present the width of solitary waves at different energy in Fig. 3 (a). The energy of solitary wave is determined by the kick strength and can be calculated with Eq. (13), where the sum is computed over the lattices on which the solitary wave is localized. At the energy E smaller than about 0.4, the width of solitary wave is relatively wide and exhibits a power-law decay with energy. At E larger than about 0.4, the decay of width becomes slower and the localization of the solitary wave becomes strong as energy increases. At $E > 50$, the solitary wave is always localized on the 4 lattices, the same as that in the pure anharmonic lattice.

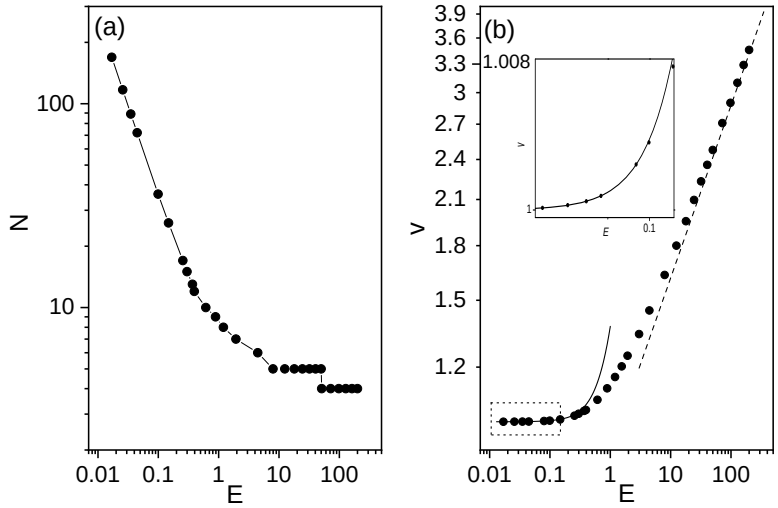

Fig. 3. The width (a) and velocity (b) *versus* the energy of solitary waves in log–log scale (dots). (a) x axis is the energy of solitary wave E and y axis is the number N of lattices where the solitary wave is localized. (b) The solid line is a fit of Eq. (17), and the dashed line is a fit of Eq. (18). The inset enlarges the region indicated by the dotted-line rectangle.

Figure 3 (b) shows the relation between energy and velocity of solitary waves in the FPU lattice. The critical value $E_c \sim 0.4$ is clearly seen in the figure. If the energy $E < E_c$, the width of solitary wave is large and the continuum approximation is applicable, so the relation is consistent with Eq. (17) [see the inset in Fig. 3 (b)]. According to Eq. (17), the velocity is only a little larger than the acoustic velocity because its energy is so small. With the increase of energy, the nonlinear part in the interaction potential of Eq. (2) becomes more and more obvious. If $E > E_c$, the solitary wave is localized on a few lattices and the long-wavelength limit is not satisfied. This leads to the deviation from the fitted curve of Eq. (17). If $E > 50$, the velocity increases with energy as a power-law function, asymptotic to $v = aE^{1/4}$ of Eq. (18) in the pure anharmonic lattice. In this case, the linear part in Eq. (2) is negligible, while the nonlinear part is significant, and the property of solitary wave becomes similar to that in the pure anharmonic lattice.

The energy of a solitary wave is the sum of kinetic energy and potential energy. A solitary wave is localized on finite lattices in the FPU model. So due to the discrete nature of the lattice, when a solitary wave is travelling on the lattice, its total energy is unchanged while its kinetic energy and potential energy vary with time periodically, as presented in Fig. 4 (a) and (b). The variation period T is the time that the solitary wave spends

on moving the distance of one lattice constant. Here, the lattice constant is unity, and then $T = 1/v$. The solitary wave with $E = 4.00$ is localized on fewer lattices and its kinetic (potential) energy has higher fluctuation than that of $E = 1.00$. To explore the fluctuations, we calculate the standard deviation σ of kinetic energy, as shown in Fig. 4 (c), which presents the transition at about $E_c \sim 0.4$. If $E < E_c$, the width of solitary wave decays with energy as a power law, and $\sigma \sim E^{10}$. If $E > E_c$, the decay of width and the increase of σ with E become slow. If E is large enough, the solitary wave is localized on 4 lattices, and σ increases linearly with E as $\sigma \sim E$, exactly like that in the pure anharmonic lattice.

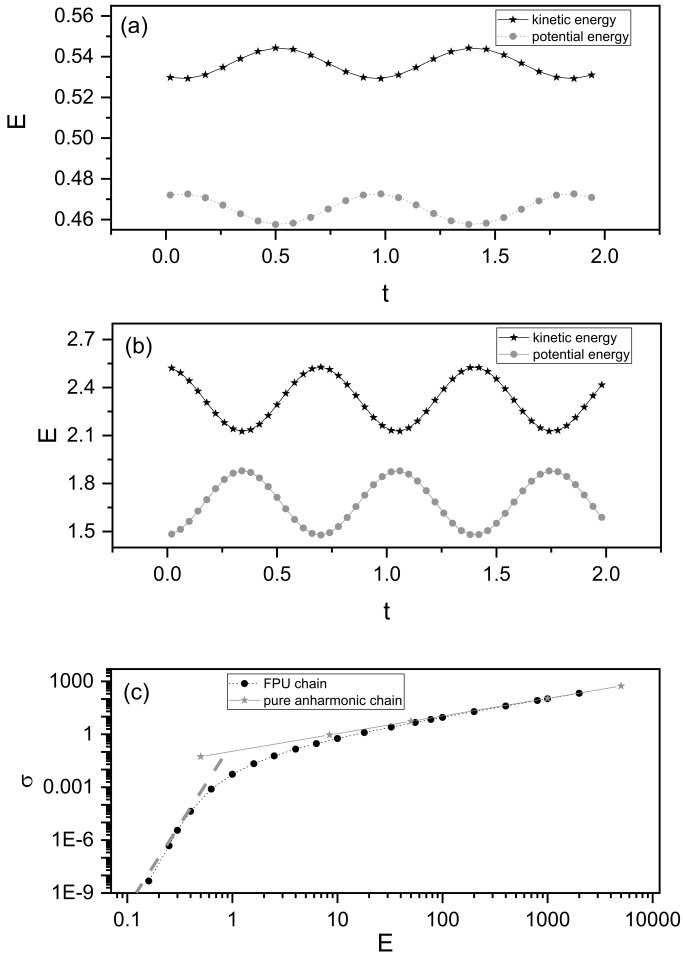

Fig. 4. (a) and (b) kinetic energy and potential energy *versus* time. Solitary wave energy $E = 1.00$ in (a) and $E = 4.00$ in (b). (c) σ *versus* E. σ is the standard deviation of kinetic energy. Dashed line is the reference to power law E^{10}.

In the following, we discuss solitary wave scattering dynamics. The solitary wave scattering is inelastic. Figure 5 shows the process of the head-on collision of a pair of solitary wave a and b. The energy of a is one half of that of b, *i.e.*, $E_a/E_b = 1/2$. Before the collision, each solitary wave maintains the shape and energy, as shown in Fig. 5 (a) and (c). After the collision, the two solitary waves, denoted as a' and b', pass through each other and the scattering behaviors are different in the following two cases. In Fig. 5 (b), both solitary waves a and b with $E_a = 0.1$ and $E_b = 0.2$ are scattered. They are scattered to a' and b' with tapered tails respectively. The energy of a and b decreases. $E_a = E_{a'} + E_{a't}$ and $E_b = E_{b'} + E_{b't}$, $E_{a't}$ is the energy of the tail of a'. In Fig. 5 (d), the scattering behavior of solitary waves with $E_a = 0.5$ and $E_b = 1.0$ is quite different from that in Fig. 5 (b). Energy exchange takes place and the scattering effect is enhanced. The large solitary wave, b, loses energy and the small one, a, gains energy, and extra wave packets are excited. Thus, the scattering effect becomes stronger with the increase of the energy of solitary wave.

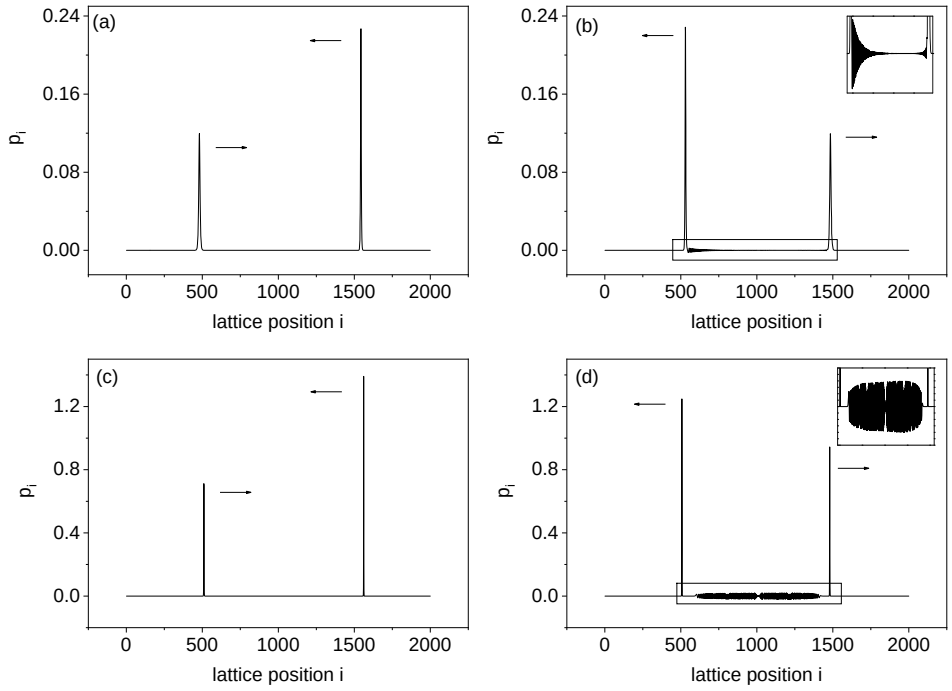

Fig. 5. Head-on collision processes of a pair of solitary wave a and b. (a) and (b) $E_a = 0.1$ and $E_b = 0.2$. (c) and (d) $E_a = 1.0$ and $E_b = 2.0$. (a) and (c) show the situation before the collision, and (b) and (d) after the collision. Insets in (b) and (d) are enlargement of rectangle.

Next, we calculate the energy fluctuation and energy loss rate of a solitary wave to describe the scattering behavior quantitatively. Due to the localization, the kinetic (potential) energy of solitary wave changes periodically with time. Then, after the collision, the scattering results vary periodically with time delay of the two solitary waves, labeled as phase δ, [16, 23] [see Fig. 6 (a)]. To show the fluctuation, in Fig. 6 (b), we calculate the standard deviation σ of $E_{b'}$, the energy of the scattered solitary wave b', with the increase of energy of b when E_a/E_b is fixed as $1/2$. It is similar to the kinetic energy fluctuation. When $E < E_c$, $\sigma \sim E^{10}$; when $E > E_c$, σ increases slowly with E; when E is large, σ varies linearly with E as $\sigma \sim E$, identical with that in the pure anharmonic lattice. For practical application, statistical properties are more significant than the prompt values. Then, we investigate the average energy loss rates, $\langle E_a - E_{a'}\rangle/E_a$ and $\langle E_b - E_{b'}\rangle/E_b$ with E as $E_a/E_b = 1/2$, shown in Fig. 6 (c) and (d).

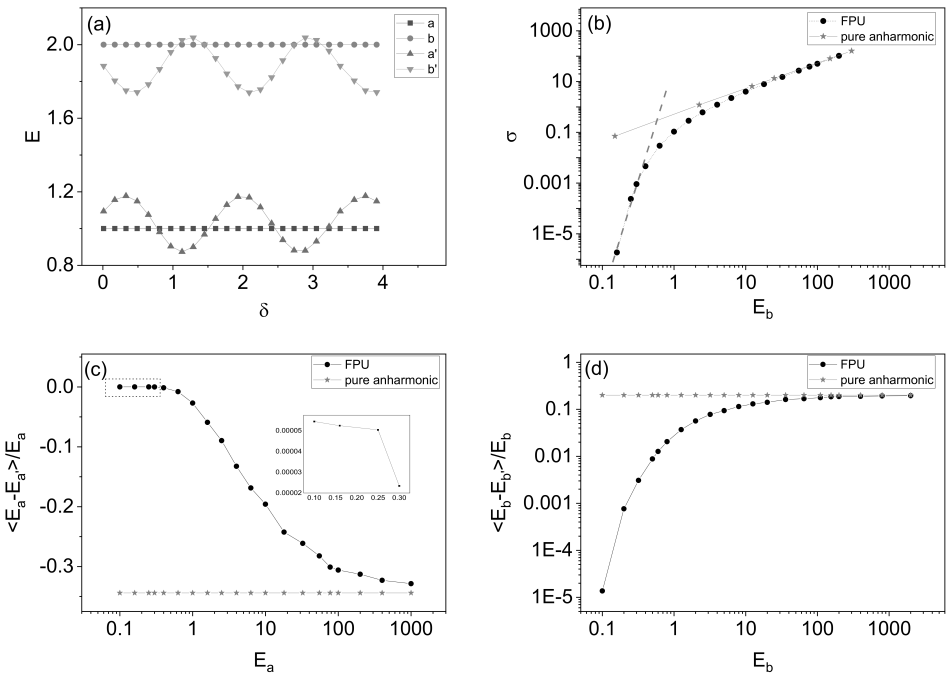

Fig. 6. (a) $E_{a'}$ and $E_{b'}$, the energy of scattered solitary wave a' and b' *versus* phase δ. $E_a = 1.0$. and $E_b = 2.0$. (b) σ of $E_{b'}$ *versus* E_b. Dashed line is the reference to power law E^{10}. (c) and (d) the average energy loss rates at $E_a/E_b = 1/2$. (c) $\langle E_a - E'_a\rangle/E_a$ *versus* E_a on a semilogarithmic scale. Inset is the enlargement of rectangle. (d) $\langle E_b - E'_b\rangle/E_b$ *versus* E_b on a log–log scale. The dot and star represent the results of solitary waves in the FPU lattice and in the pure anharmonic lattice, respectively.

The scattering results show the critical value is also $E_c \sim 0.4$. When $E < E_c$, the energy loss rates of a and b are more than 0, *i.e.*, both a and b lose energy. The scattering process can be approximately shown by Fig. 5 (a) and (b). Both of the two solitary waves are scattered into smaller ones with tapered tails and there is no energy exchange between them. The scattering effect is quite weak as the loss rate is quite small. In Fig. 6 (d), the energy loss rate of b indicates a power-law increase with E. When $E > E_c$, the energy loss rate is less than 0 for the small solitary wave a and is more than 0 for the large solitary wave b. The scattering process is similar to that in Fig. 5 (c) and (d). There is an energy exchange between the two solitary waves, *i.e.*, large solitary wave b loses energy and small one, a, obtains energy on average, and extra wave packets are excited. With the increase of energy, solitary wave localization is more robust, and the energy loss rate of large solitary wave b increases more slowly, see Fig. 6 (d). The stars in Fig. 6 are the scattering results for the pure anharmonic lattice. Any pair of solitary waves with the same ratio E_a/E_b has the same loss rates due to the scaling property [16]. In the FPU lattice, the scattering results approach those in the pure anharmonic lattice when $E \to \infty$.

Discrete breathers are time-periodic and spatially localized nonlinear excitations in nonlinear systems, and have been experimentally observed and investigated in different media such as granular crystals, electrical lattices, optical waveguides and photonic crystals, the Bose–Einstein condensation, and so on [24–28]. On the FPU lattice, the discrete breathers can be excited by applying a displacement kick to the middle lattice for a static system. Then we discuss the scattering dynamics of solitary wave and discrete breather quantitatively.

Figures 7 (a) and (b) show the collision process of a solitary wave a and a discrete breather b. $E_a = 0.89$ and $E_b = 0.51$. The solitary wave travels towards the discrete breather and the discrete breather is immobile. After the collision, the solitary wave passes through the discrete breather, and the position of the discrete breather shifts a little. Both solitary wave a and discrete breather b are scattered. Solitary wave a and discrete breather b are scattered to a' and b' and both energies of a and b decrease. Since the lattice is discrete and the solitary wave and discrete breather are localized, the scattering results vary periodically with phase δ as well. Then, we calculate the energy fluctuation, the standard deviation σ of energy of scattered solitary wave a', $E_{a'}$, and the average energy loss rate of solitary wave a, $\langle E_a - E_{a'} \rangle / E_a$. Figures 7 (c) and (d) show the interaction results between discrete breather b and solitary wave a with different energies, and the two lines represent the energy of discrete breather $E_b = 0.51$ and $E_b = 1.05$, respectively. The curve of σ of $E_{a'}$ in Fig. 7 (c) indicates the transitional zone of solitary wave at E_c as well. When $E < E_c$, σ increases as power law

with E; when $E > E_c$, σ varies slowly with E. This reflects the transition of localization of solitary wave at E_c. In Fig. 7 (d), the energy loss rate of solitary wave first increases and then decreases with E and the transition is not E_c anymore. The interaction between solitary wave and discrete breather is more complicated, which is determined by the properties of not only solitary wave but also discrete breather.

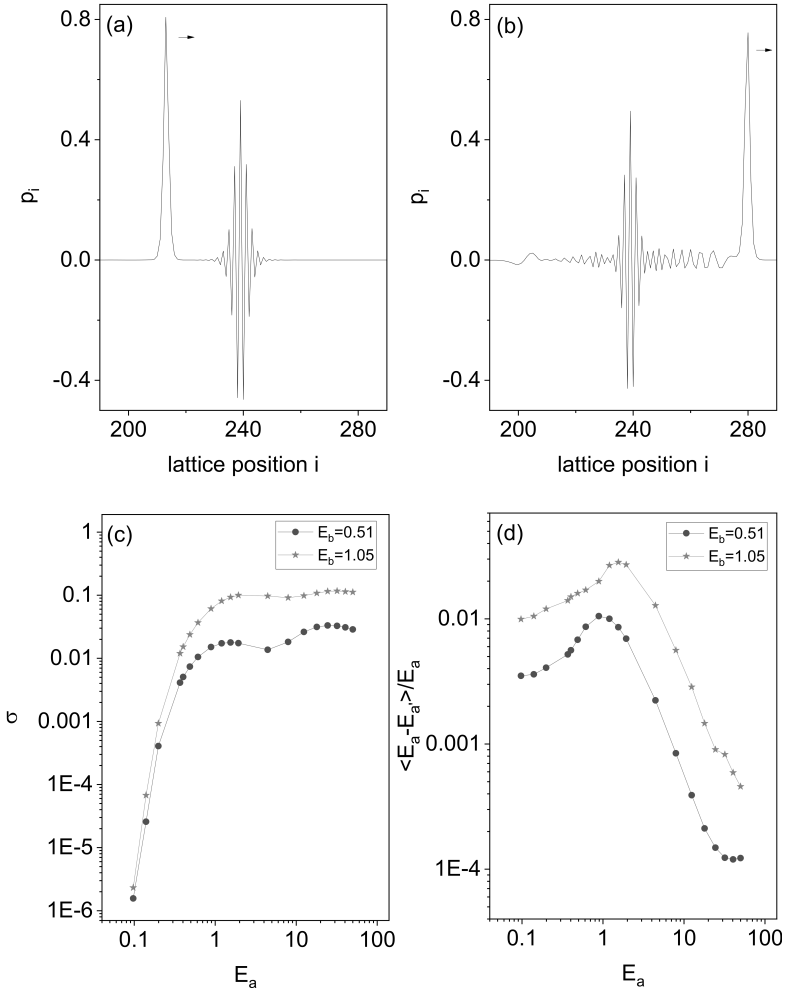

Fig. 7. (a) and (b) the collision process of a solitary wave a and a discrete breather b. $E_a = 0.89$ and $E_b = 0.51$. (a) and (b) show the situation before and after collision. (c) the standard deviation σ of $E_{a'}$ *versus* E_a on a log–log scale. (d) the average energy loss rate of solitary wave a, $\langle E_a - E'_a \rangle / E_a$ *versus* E_a on a log–log scale. The dot and star represent the energy of discrete breather $E_b = 0.51$ and $E_b = 1.05$, respectively.

5. Conclusion and discussion

In summary, we explore the solitary wave transition from low to high energy in the FPU lattice. If energy is smaller than the energy threshold $E_c \sim 0.4$, the continuum approximation is applicable, so the relation of energy and velocity of a solitary wave is consistent with analytical results. The width of solitary wave decays as power law as energy increases. When a solitary wave propagates, kinetic energy and potential energy are varying periodically, while the total energy does not change. The fluctuation of kinetic (potential) energy increases with energy as power law. After a head-on collision of two solitary waves, the energy loss rate of large solitary wave shows a power-law increase with energy. After scattering of a solitary wave and a discrete breather, the energy fluctuation of the solitary wave increases as power law with energy. If energy is larger than the threshold E_c, analytical solutions are not applicable anymore. The properties mentioned above vary more slowly. If the energy is large enough, the properties of solitary waves tend to those in the pure anharmonic lattice.

The chaotic dynamics of the FPU lattice are quite different between below and above a critical value ε_c of energy density ε. The degree of chaoticity of the dynamics can be quantified by the largest Lyapunov exponent λ, which is a measure of the average rate of local exponential separation between nearby trajectories in phase space. $\lambda \sim \varepsilon^2$ for $\varepsilon < \varepsilon_c$ and $\lambda \sim \varepsilon^{2/3}$ for $\varepsilon > \varepsilon_c$ [29, 30]. This reflects the transition of solitary wave from a low to high energy since solitary waves are the dominant excitations. We discuss it with the concept of solitary wave scattering. If $E > E_c$, the scattering effect increases with energy as power law, while for $E < E_c$ it slowly increases. This is in agreement with the chaotic behavior.

This work is supported by the National Natural Science Foundation of China under grant No. 10805034.

REFERENCES

[1] J.S. Russell, «Report on Waves, Report of the Meeting of the British Association for the Advancement of Science», *John Murray*, London 1844.

[2] D.J. Korteweg, G. de Vries, «XLI. On the change of form of long waves advancing in a rectangular canal, and on a new type of long stationary waves», *Philos. Mag.* **39**, 422 (1895).

[3] E. Fermi, J. Pasta, S. Ulam, «Studies of Nonlinear Problems», Los Alamos Document No. LA-1940, 1955.

[4] N.J. Zabusky, M.D. Kruskal, «Interaction of "Solitons" in a Collisionless Plasma and the Recurrence of Initial States», *Phys. Rev. Lett.* **15**, 240 (1965).

[5] A.C. Scott, «Nonlinear Science», *Oxford University Press*, New York 1999.

[6] A.C. (Ed.) «The Encyclopedia of Nonlinear Science», *Routledge*, New York 2005.

[7] A. Vainchtein, «Rarefactive lattice solitary waves with high-energy sonic limit», *Phys. Rev. E* **102**, 052218 (2020).

[8] H. Sakaguchi, K. Ishibashi, «Flip motion of solitary wave in an Ising-type Vicsek model», *Phys. Rev. E* **100**, 052113 (2019).

[9] S. Katz, S. Givli, «Solitary waves in a nonintegrable chain with double-well potentials», *Phys. Rev. E* **100**, 032209 (2019).

[10] M. Hwang, A.F. Arrieta, «Solitary waves in bistable lattices with stiffness grading: Augmenting propagation control», *Phys. Rev. E* **98**, 042205 (2018).

[11] A. Vainchtein, Y. Starosvetsky, J.D. Wright, R. Perline, «Solitary waves in diatomic chains», *Phys. Rev. E* **93**, 042210 (2016).

[12] V.I. Kruglov, H. Triki, «Periodic and solitary waves in an inhomogeneous optical waveguide with third-order dispersion and self-steepening nonlinearity», *Phys. Rev. A* **103**, 013521 (2021).

[13] R.Y. Ondoua, D.B. Belobo, «Solitary waves dynamic for Davydov α-helical protein model: Effects of localized and periodic inhomogeneities», *Phys. Rev. E* **102**, 062414 (2020).

[14] M. Remoissenet, «Waves Called Solitons», *Springer Berlin Heidelberg*, Berlin, Heidelberg 1999.

[15] B. Hu, B. Li, H. Zhao, «Heat conduction in one-dimensional nonintegrable systems», *Phys. Rev. E* **61**, 3828 (2000).

[16] H. Zhao, Z. Wen, Y. Zhang, D. Zheng, «Dynamics of Solitary Wave Scattering in the Fermi–Pasta–Ulam Model», *Phys. Rev. Lett.* **94**, 025507 (2005).

[17] Y.A. Kosevich, «Nonlinear envelope-function equation and strongly localized vibrational modes in anharmonic lattices», *Phys. Rev. B* **47**, 3138 (1993).

[18] P. Poggi, S. Ruffo, H. Kantz, «Shock waves and time scales to reach equipartition in the Fermi–Pasta–Ulam model», *Phys. Rev. E* **52**, 307 (1995).

[19] R. Khomeriki, «Interaction of a kink soliton with a breather in a Fermi–Pasta–Ulam chain», *Phys. Rev. E* **65**, 026605 (2002).

[20] M.J. Ablowitz, H. Segur, «Solitons and the Inverse Scattering Transform», *SIAM*, Philadelphia 1981.

[21] M.J. Ablowitz, P.A. Clarkson, «Solitons, Nonlinear Evolution Equations and Inverse Scattering», *Cambridge University Press*, Cambridge 1991.

[22] J. Szeftel, P. Laurent-Gengoux, E. Ilisca, «Anharmonicity-Induced Solitons in One-Dimensional Periodic Lattices», *Phys. Rev. Lett.* **83**, 3982 (1999).

[23] Z. Wen, H. Zhao, «Different Types of Solitary Wave Scattering in the Fermi–Pasta–Ulam Model», *Chin. Phys. Lett.* **22**, 1340 (2005).

[24] A.P. Chetverikov, W. Ebeling, V.D. Lakhno, M.G. Velarde, «Discrete-breather-assisted charge transport along DNA-like molecular wires», *Phys. Rev. E* **100**, 052203 (2019).

[25] Y.Y. Yamaguchi, Y. Doi, «Low-frequency discrete breathers in long-range systems without on-site potential», *Phys. Rev. E* **97**, 062218 (2018).

[26] D. Saadatmand *et al.*, «Discrete breathers assist energy transfer to ac-driven nonlinear chains», *Phys. Rev. E* **97**, 022217 (2018).

[27] S.P. Wallen *et al.*, «Discrete breathers in a mass-in-mass chain with Hertzian local resonators», *Phys. Rev. E* **95**, 022904 (2017).

[28] I. Evazzade *et al.*, «Energy transfer in strained graphene assisted by discrete breathers excited by external ac driving», *Phys. Rev. B* **95**, 035423 (2017).

[29] M. Pettini, M. Landolfi, «Relaxation properties and ergodicity breaking in nonlinear Hamiltonian dynamics», *Phys. Rev. A* **41**, 768 (1990).

[30] M. Pettini, M. Cerruti-Sola, «Strong stochasticity threshold in nonlinear large Hamiltonian systems: Effect on mixing times», *Phys. Rev. A* **44**, 975 (1991).